RESEARCH PAPER

Channels 5:1, 1-16; January/February 2011; © 2011 Landes Bioscience

Open- and closed-state fast inactivation in sodium channels

Differential effects of a site-3 anemone toxin

James R. Groome,[1,*] Boris D. Holzherr[2] and Frank Lehmann-Horn[2]

[1]Department of Biological Sciences; Idaho State University; Pocatello, ID USA; [2]Division of Neurophysiology; Ulm University; Ulm, Germany

Key words: anthopleurin, charge immobilization, fast inactivation, sodium channel, voltage-gated

Abbreviations: Ap-A, anthopleurin-A; DIS4, domain one, transmembrane segment four; DIIS4, domain two, transmembrane segment four; DIIIS4, domain three, transmembrane segment four; DIVS4, domain four, transmembrane segment four; $hNa_V1.4$, human skeletal muscle voltage gated sodium channel; IFMT, isoleucine phenylalanine methionine threonine; TTX, tetrodotoxin

The role of sodium channel closed-state fast inactivation in membrane excitability is not well understood. We compared open- and closed-state fast inactivation, and the gating charge immobilized during these transitions, in skeletal muscle channel $hNa_V1.4$. A significant fraction of total charge movement and its immobilization occurred in the absence of channel opening. Simulated action potentials in skeletal muscle fibers were attenuated when pre-conditioned by subthreshold depolarization. Anthopleurin A, a site-3 toxin that inhibits gating charge associated with the movement of DIVS4, was used to assess the role of this voltage sensor in closed-state fast inactivation. Anthopleurin elicited opposing effects on the gating mode, kinetics and charge immobilized during open- versus closed-state fast inactivation. This same toxin produced identical effects on recovery of channel availability and remobilization of gating charge, irrespective of route of entry into fast inactivation. Our findings suggest that depolarization promoting entry into fast inactivation from open versus closed states provides access to the IFMT receptor via different rate-limiting conformational translocations of DIVS4.

Introduction

Sodium channels are the critical determinant of the excitatory, rising phase of the action potential.[1,2] Sodium flux through these channels provides the depolarizing influence to generate action potentials, and is regulated by voltage-dependent transitions between closed, open and inactivated states of the protein. Action potential frequency in excitable cells such as neurons, cardiac and skeletal muscle fibers dictate the nature of information flow. Sodium channel inactivation and its recovery are critical determinants of action potential frequency. Fast inactivation of the channel in response to membrane depolarization occurs on a time scale of ms, whereas several forms of slow inactivation occur with prolonged depolarization. Defective inactivation is a hallmark of mutations identified in brain and muscle diseases, so called channelopathies, underscoring the critical importance of this function of sodium channels in excitable cells.[3-5]

The observation that sodium channels can inactivate without opening[6,7] has been followed by relatively few investigations into the structural basis of this process. Nevertheless, studies of sodium channel mutations in diseases of cardiac[8-10] or skeletal[11-14] muscle have shown that these mutations disrupt closed-state fast inactivation. Therefore, a more complete understanding of this form of fast inactivation is needed to provide insight into diseases of excitability in neurons and muscle fibers.

The inactivation particle in sodium channels has been identified as a conserved IFMT motif in the cytoplasmic region linking domains III and IV.[15,16] Voltage dependence in sodium channel gating is ascribed to the movement of homologous S4 segments of the sodium channel[17] as supported by a diversity of experimental approaches. Unequal charge content of S4 segments in the 4 domains[18] suggests that voltage sensors have domain-specific functions. For example, translocation of DIVS4 permits access to the receptor for the inactivation particle following channel opening.[19,20] In the present work we tested the hypothesis that DIVS4 regulates inactivation in the absence of channel opening. To do this we used the polypeptide site-3 toxin anthopleurin, known to inhibit the movement of this voltage sensor.[21]

With open-state fast inactivation, a significant fraction of the gating charge carried by voltage sensor movement becomes immobilized.[22] During repolarization of membrane potential, return of voltage sensors (charge remobilization) and unbinding of the inactivation particle are key determinants of membrane excitability, at least in terms of information coded by repetitive

*Correspondence to: James R. Groome; Email: groojame@isu.edu
Submitted: 07/18/10; Revised: 10/08/10; Accepted: 10/26/10
Previously published online: www.landesbioscience.com/journals/channels/article/14031

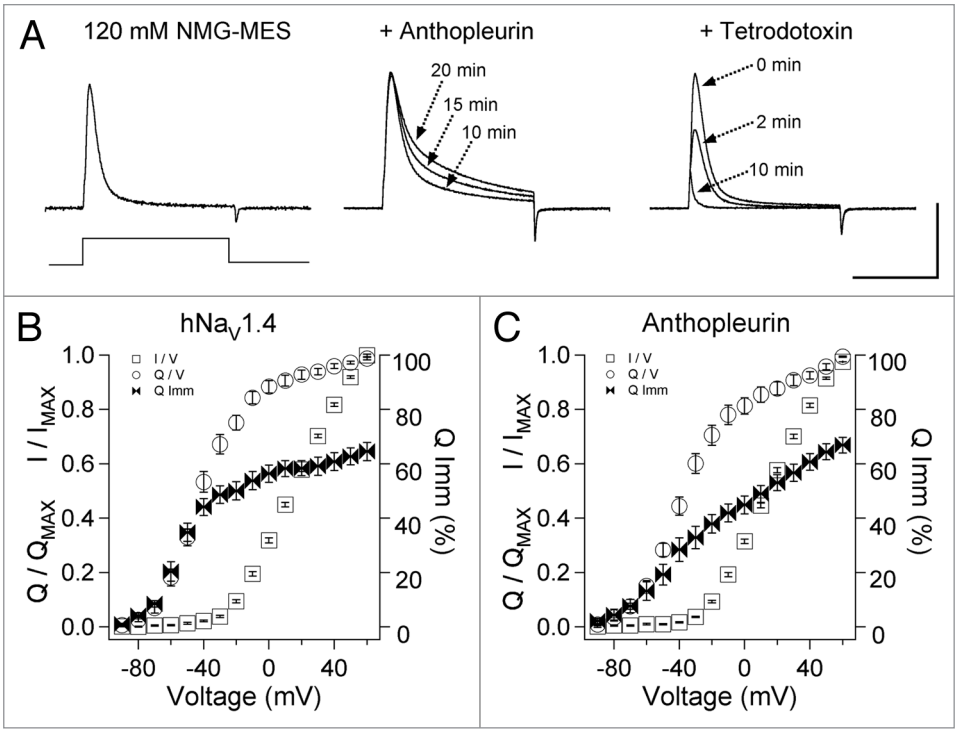

Figure 1. (A) Ionic and gating currents of $hNa_V1.4$ in the cut-open configuration in response to 0 mV depolarization for control (left), 500 nM anthopleurin (middle) or 2 μM tetrodotoxin (right). Parameters for conductance, charge movement and its immobilization were obtained from Boltzmann fits to normalized curves as shown in (B and C). Values represent mean ± SEM for 16 to 34 experiments. Calibration: vertical 400 nA; horizontal 10 ms.

Table 1. Equilibrium parameters for ionic and gating currents in naïve and anthopleurin-modified channels

Parameters, Ionic current	$hNa_V1.4$	500 nM anthopleurin
Midpoint of Activation (mV)	16.8 ± 0.69 (37)	18.0 ± 0.88 (39)
Activation Slope	1.45 ± 0.02	1.45 ± 0.03
Midpoint of Inactivation (mV)	-63.8 ± 0.70 (17)	-64.2 ± 0.72 (12)
Inactivation Slope Factor	-4.67 ± 0.15 (17)	-3.08 ± 0.16 (15)***
Iss/Ipeak, 300 ms	1.15 ± 0.25% (19)	3.19 ± 0.36% (11)***
Parameters, Gating Current		
Midpoint of Charge Moved (mV)	-40.4 ± 1.64 (26)	-34.4 ± 3.86 (22)
Charge Moved Slope Factor	2.22 ± 0.26	1.92 ± 0.24
Midpoint of Charge Immobilized (mV)	-47.9 ± 3.75	-28.6 ± 4.96**
Charge Immobilization Slope Factor	1.93 ± 0.14	1.05 ± 0.10***

**p ≤ 0.005. ***p ≤ 0.0001.

action potentials. Voltage sensors in domains III and IV carry the immobilizable fraction of gating charge[23] and remobilization of gating charge in DIVS4 following open-state fast inactivation dictates the return of channels to an available state.[24,25] Translocations of voltage sensors in domains III and IV appear to be requisite for sodium channels to inactivate from closed states.[26,27] However, the extent to which these voltage sensors are immobilized during closed-state fast inactivation has not been investigated. Therefore, we decided to quantify gating charge immobilization during closed-state fast inactivation, and determine its impact to limit the recovery of channel availability following inactivation.

In the present study we compared onset and recovery parameters of channel availability and charge immobilization for open- and closed-state fast inactivation. Ultimately we sought to determine whether weak depolarization, insufficient to open channels, produces a state of inactivation that is functionally similar to that achieved with stronger depolarization that activates channels. Our findings with voltage clamp experiments and computer simulation show that closed-state fast inactivation has a significant impact on membrane excitability. Then, we used the site-3 toxin anthopleurin-A to determine the role of DIVS4 in these two routes to fast inactivation. This toxin prolonged fast inactivation and the immobilization of gating charge from the open state, but accelerated these parameters during closed-state transitions. Recovery and remobilization of the gating charge in channels inactivating from open or closed states were accelerated by anthopleurin. The action of a site-3 toxin to enhance, rather than inhibit, closed-state inactivation of channels suggests that binding of anthopleurin favors an intermediate position of DIVS4. Some of these results have been reported in abstract form.[28]

Results

Charge movement and immobilization. Ionic and gating currents were recorded from oocytes expressing wild type $hNa_V1.4$ α

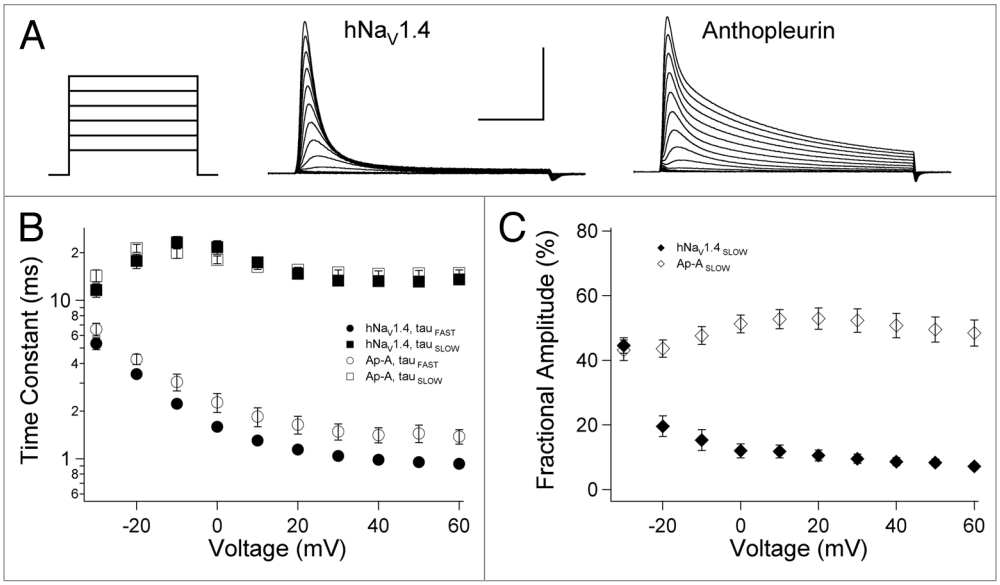

Figure 2. Open-state fast inactivation. (A) Channels were depolarized to voltages ranging from -90 mV to 60 mV for naïve or anthopleurin-modified channels. Decays in ionic current were fit with the sum of two exponentials to yield parameters for kinetics (B) and gating mode (C) describing FAST and SLOW components. Values represent mean ± SEM for 33 to 34 experiments. Calibration: vertical 1 μA; horizontal 5 ms.

subunit and β_1 subunit, using the cut-open oocyte configuration. To optimize voltage control and to facilitate recordings of gating current, 120 mM NMG-MES was used for the external, bath solution. In **Figure 1A**, outward currents in response to 0 mV depolarization from a holding potential of -120 mV are shown for naïve and toxin-modified channels. Anthopleurin-A was added at 500 nM, with its effect on fast inactivation saturating after 20 min. Tetrodotoxin (TTX) was added at 2 μM to isolate gating currents (arrow at 10 min shows ON gating current) in recordings of naïve or anthopleurin-modified channels.

For each of the treatments in **Figure 1A**, channels were depolarized to voltages ranging from -90 mV to 60 mV to compare conductance (I/V), charge movement (Q/V) and charge immobilization (Q Imm/V), with the normalized curves shown in **Figure 1B and C**. Parameters were determined from Boltzmann fits, and are presented in **Table 1.** Since threshold of activation was -30 mV for naïve or anthopleurin-modified channels, we defined voltage ranges over which closed-state fast inactivation would occur as -40 mV or more negative, and for open-state fast inactivation as -30 mV or more positive. The midpoint of charge moved ($Q/V_{1/2}$) was left-shifted by approximately 50 mV compared to that for the I/V curve, such that even with short depolarizing pulses of 20 ms, charge movement through closed states was readily quantified.

In TTX-modified channels, charge moved and was immobilized with steep voltage dependence at voltages of -40 mV or more negative. From -40 mV to 0 mV, charge moved with a voltage dependence greater than that observed for charge immobilization. At more depolarized potentials (0 mV to 60 mV), voltage dependencies for charge movement and its immobilization were shallow. Depolarization to -40 mV promoted 51.3% of total gating charge movement (Q_{MAX}). At this voltage, 45.7% of Q_{MAX} was immobilized, corresponding to 66.0% of the immobilizable fraction. Thus, depolarization without activation of channels moved and immobilized a large fraction of the total gating charge.

Anthopleurin did not significantly alter midpoint or slope factor for the curves describing I/V or Q/V relations (**Table 1**). However, the toxin produced two significant effects on charge immobilization (Q Imm, **Table 1**). First, the midpoint of charge immobilization (Q $Imm/V_{1/2}$) was right-shifted (-28.6 mV), compared to channels exposed only to TTX (-47.9 mV). Second, anthopleurin decreased slope factor for this curve. In a separate set of experiments (n = 7), anthopleurin was added after TTX block, to quantify anthopleurin-mediated reduction in Q_{MAX} for these recording conditions. At 20 min exposure to toxin, Q/Q_{MAX} was decreased in the voltage range for closed-state transitions (-80 mV to -50 mV) by 2.13 ± 0.1% and by 29.8 ± 0.4% at voltages from 30 mV to 60 mV. This effect of anthopleurin to reduce Q_{MAX} at depolarized voltages was similar to that reported for anthopleurin on $rNa_V1.4$ (33%) expressed in mammalian cells,[29] and for α (site-3) scorpion toxin Ts3 on $rNa_V1.4$ (30%) expressed in oocytes and recorded at 14°C in the cut-open configuration.[30]

Open-state fast inactivation and charge immobilization. We determined the kinetics and gating mode of open-state fast inactivation in naïve and anthopleurin-modified channels. In experiments as shown in **Figure 2A**, fast inactivation followed a bi-exponential time course at voltages ranging from -30 mV to 60 mV. Decays in ionic current at these voltages were fit with the sum of two exponentials to yield parameters describing the kinetics (**Fig. 2B**) and fractional amplitudes (**Fig. 2C**) for the FAST and SLOW components (gating modes) of inactivation.

To determine the kinetics for charge immobilizing during open-state fast inactivation, ON and OFF gating currents were elicited from TTX- or TTX/anthopleurin-modified channels with step commands of variable voltage and duration as shown in **Figure 3A**. Percent charge immobilized was determined for

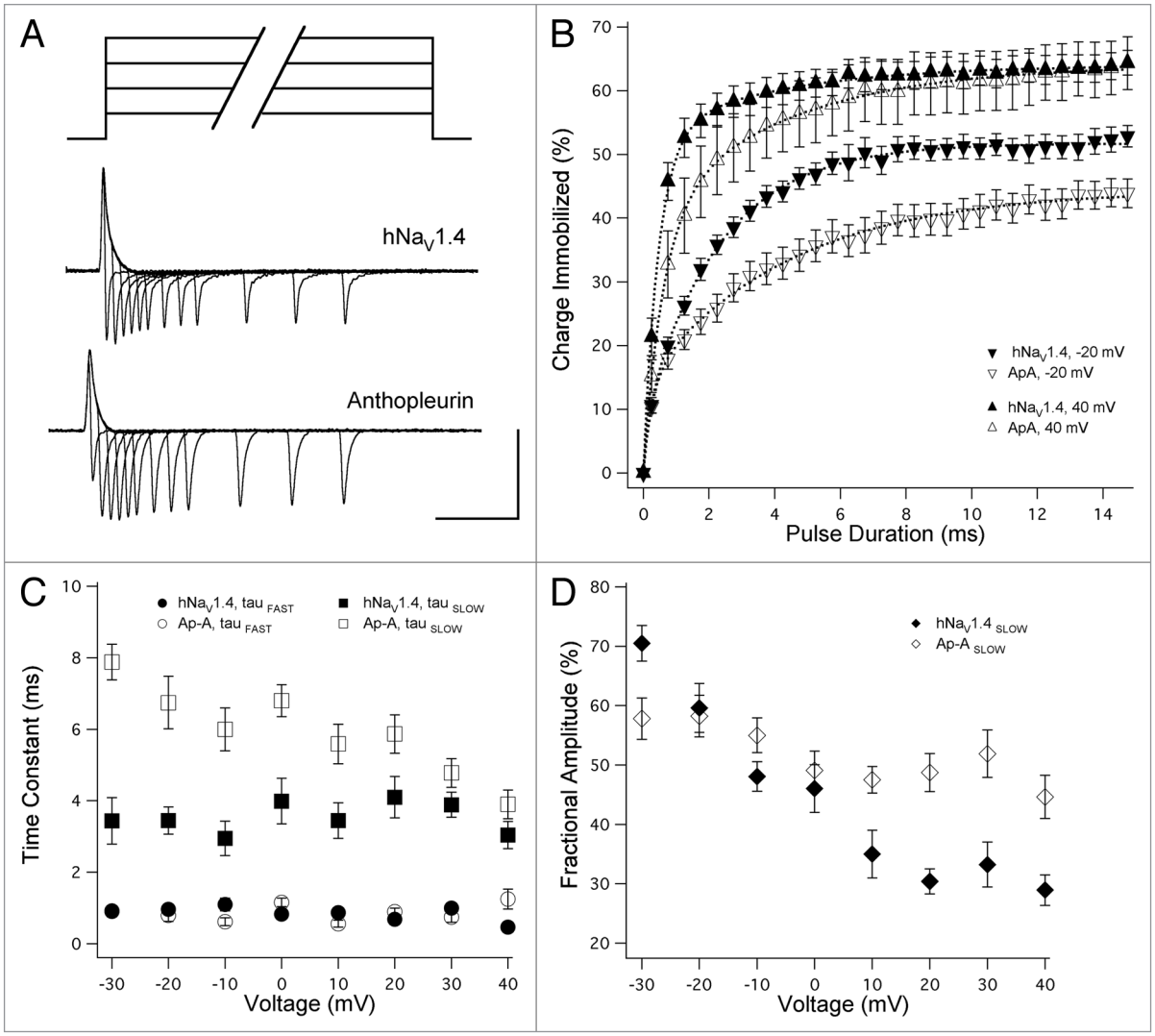

Figure 3. Open-state charge immobilization. (A) TTX- or TTX/anthopleurin-modified channels were depolarized with variable voltage (0 mV shown in traces) and duration pulses to elicit ON and OFF gating currents. (B) Onset of charge immobilization with select voltages shown. These curves were used to calculate parameters of kinetics (C) and fractional amplitudes (D) of FAST and SLOW phases of immobilization. Values represent mean ± SEM for 20 to 25 experiments. Calibration: vertical 200 nA; horizontal 5 ms.

pulse durations up to 15 ms (**Fig. 3B**). FAST and SLOW phases of charge immobilization were apparent from these curves, which were fit with the sum of two exponentials. In **Figure 3C**, onset kinetics for charge immobilized are plotted as a function of command voltage. Time constants describing the FAST phase of immobilization were similar for TTX- and TTX/anthopleurin-modified channels. However, anthopleurin significantly increased time constants describing the SLOW phase of immobilization across a voltage range of -30 mV to 30 mV, with a mean increase of 75.2% in time constants.

A steep voltage dependence was observed in the fractional amplitudes describing the two phases of charge immobilization. As shown in **Figure 3B and D**, more positive depolarization of channels into the open state decreased the fractional amplitude of the SLOW phase of charge immobilization. For channels exposed to both TTX and anthopleurin, this voltage dependence was attenuated. At -30 mV, the fractional amplitude of the SLOW phase of charge immobilization was significantly decreased in these channels, but was increased at voltages more positive than 0 mV.

Closed-state fast inactivation and charge immobilization. We hypothesized that closed-state fast inactivation regulates membrane excitability by immobilizing the gating charge and limiting the pool of sodium channels available for activation. To test that hypothesis, we used protocols in which pre-pulse conditioning depolarization was limited to voltage commands that do not activate channels. Channels were inactivated at voltages ranging from -90 mV to -40 mV, for durations ranging from 0 to 300 ms. We then tested for channel availability with 0 mV test pulses following each pre-pulse (**Fig. 4**). After TTX block, this protocol was used to determine charge immobilization during closed-state fast inactivation. To do this, we measured the magnitude of the ON gating charge elicited by 0 mV test pulses following each pre-pulse (**Fig. 5**).

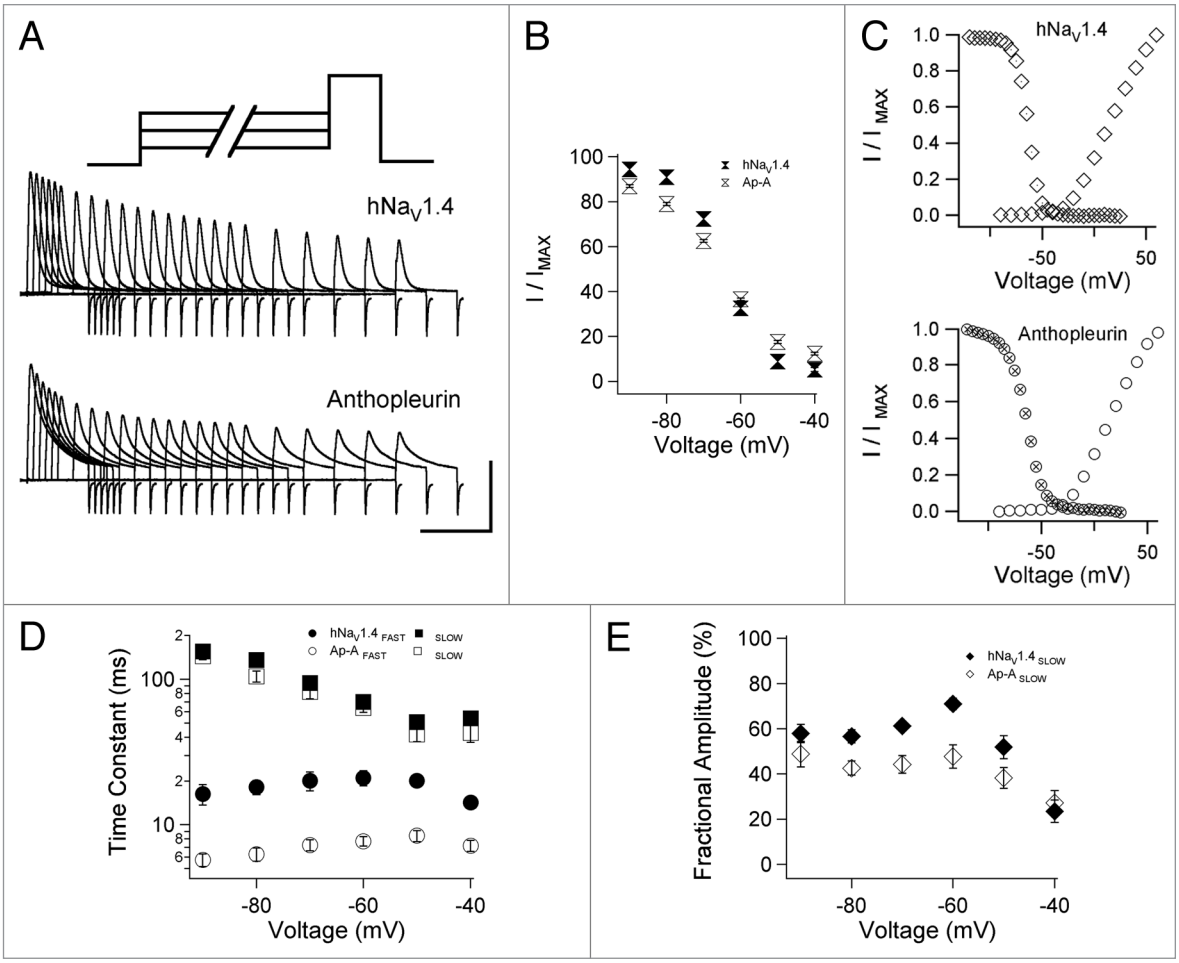

Figure 4. Closed-state fast inactivation. (A) Channels were depolarized for durations up to 300 ms and tested for availability with a test pulse to 0 mV. (B) Availability curves for naïve and anthopleurin-modified channels. (C) Steady-state inactivation curves (300 ms pre-pulses) and I/V relations. Kinetics (D) and fractional amplitudes (E) for FAST and SLOW components of closed-state fast inactivation. Values represent mean ± SEM for 20 to 23 experiments (B, D and E) or 12 to 17 experiments for steady-state fast inactivation (C). Calibration: vertical 400 nA; horizontal 10 ms.

Figure 4A shows the gradual decrease in ionic current elicited from test pulses that followed -60 mV conditioning pre-pulses of increasing duration. For each conditioning voltage, we plotted the current at time t normalized to the maximum current at time zero, as a function of pre-pulse duration. These curves were fit with a double exponential function to yield the parameters shown in **Figure 4B, D and E**. Anthopleurin significantly increased the extent of inactivation at voltages from -90 to -70 mV and decreased inactivation at -50 mV and -40 mV, compared to naïve channels. These findings were in agreement to those obtained in separate experiments showing that toxin decreased the slope factor of the steady-state fast inactivation (h∞) curve (**Fig. 4C and Table 1**). By plotting h∞ and I/V curves together, it was apparent that site-3 toxin did not promote a large window current of activation in the absence of fast inactivation.

As done for open-state fast inactivation, kinetics and fractional amplitudes of the two components describing closed-state fast inactivation were determined for naïve and anthopleurin-modified channels. Site-3 toxin significantly accelerated the FAST component of closed-state fast inactivation at all voltages tested, with a mean reduction in time constant of 60.9% (**Fig. 4D**). Kinetics describing the SLOW component were unaffected by toxin. Fractional amplitudes of the two components were not steeply voltage dependent, except at voltages near activation threshold (**Fig. 4E**). Compared to naïve channels, anthopleurin significantly decreased the fractional amplitude of the SLOW component over the voltage range of -80 mV to -60 mV, where inactivation is predominantly from closed states.

We then determined the extent and kinetics of charge immobilization during closed-state fast inactivation. **Figure 5A** shows the decrease in Ig_{ON} in response to 0 mV test pulses following conditioning pre-pulses to -60 mV of increasing duration, for TTX- or TTX/anthopleurin-modified channels. Integrals for Ig_{ON} tested after each conditioning pre-pulse were normalized to Ig_{ON} at zero pre-pulse duration, and the normalized curves were fit with the sum of two exponentials. At voltages near activation threshold, approximately two-thirds of the gating charge was immobilized in the absence of channel opening (**Fig. 5B**). Thus, when long duration conditioning pulses were employed to inactivate channels from the closed state, the extent of charge

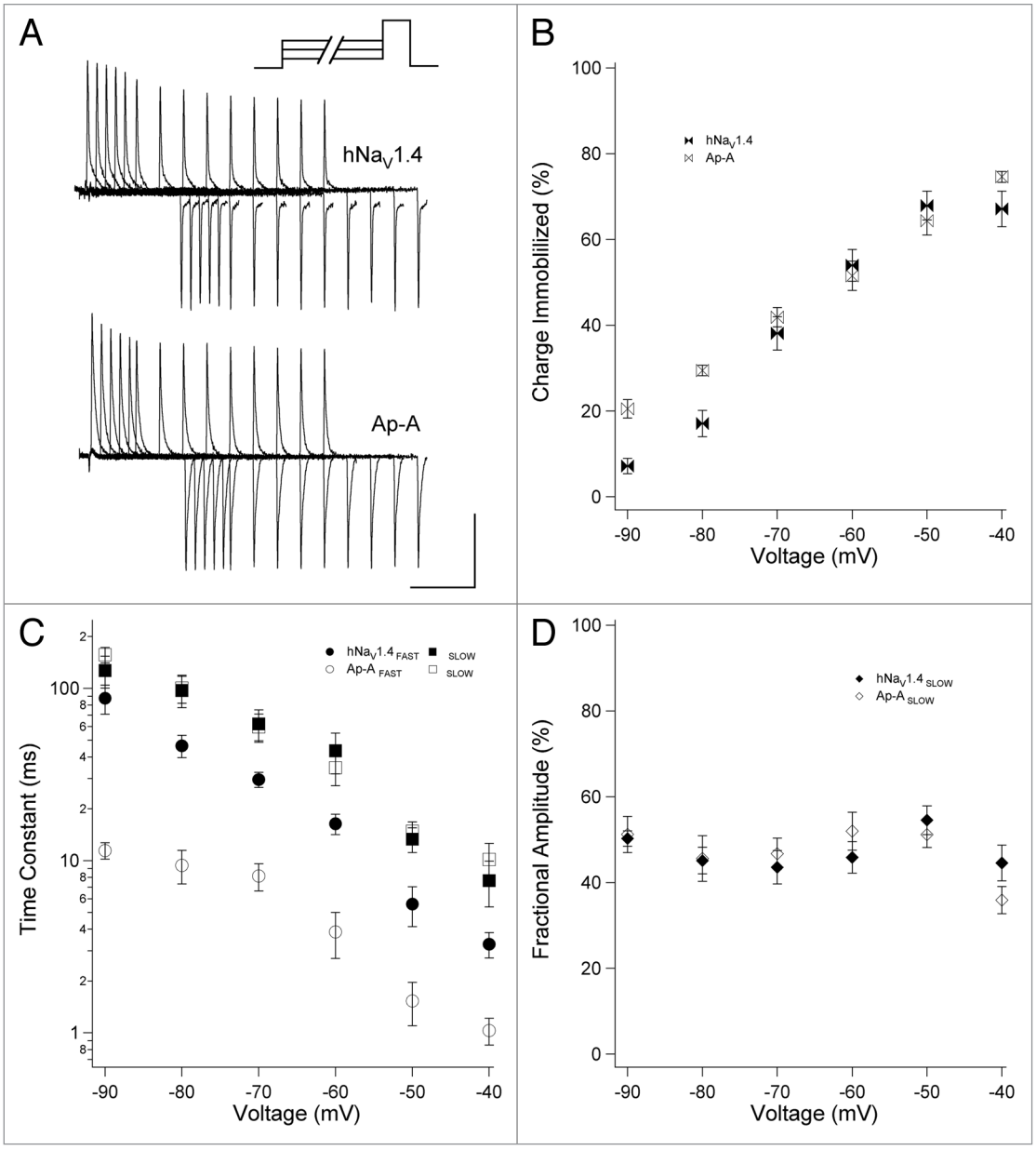

Figure 5. Closed-state charge immobilization. (A) TTX- or TTX/anthopleurin-modified channels were conditioned with variable voltage pulses (-60 mV prior to these traces) and tested with 0 mV pulses to generate ON gating currents. Normalized curves of Ig_{ON} versus pre-pulse duration were used to calculate parameters of extent (B), kinetics (C) and fractional amplitudes (D) of charge immobilization. Values represent mean ± SEM for 12 to 14 experiments. Calibration: vertical 200 nA; horizontal 5 ms.

immobilized approximated that observed during open-state fast inactivation.

Kinetics of closed-state charge immobilization were described by FAST and SLOW phases (**Fig. 5C**). For charge immobilization over the voltage range for closed-state fast inactivation, steep voltage dependence was observed for the kinetics of each phase (**Fig. 5C**). Anthopleurin significantly accelerated the FAST phase of charge immobilization at all voltages tested, but did not alter kinetics of the SLOW phase of charge immobilization. Fractional amplitudes of gating charge immobilization were independent of pre-pulse conditioning voltage and were unaffected by site-3 toxin (**Fig. 5D**).

Taken together, the findings from the experiments shown in **Figure 2** through **Figure 4** indicated that anthopleurin produced effects on inactivation and charge immobilization dependent on the route of entry into the fast-inactivated state. Site-3 toxin slowed the kinetics of fast inactivation and charge immobilization for channels that opened, and increased the fraction of channels gating in a SLOW mode of inactivation. In contrast, anthopleurin accelerated fast inactivation and immobilization of gating charge in closed channels. However,

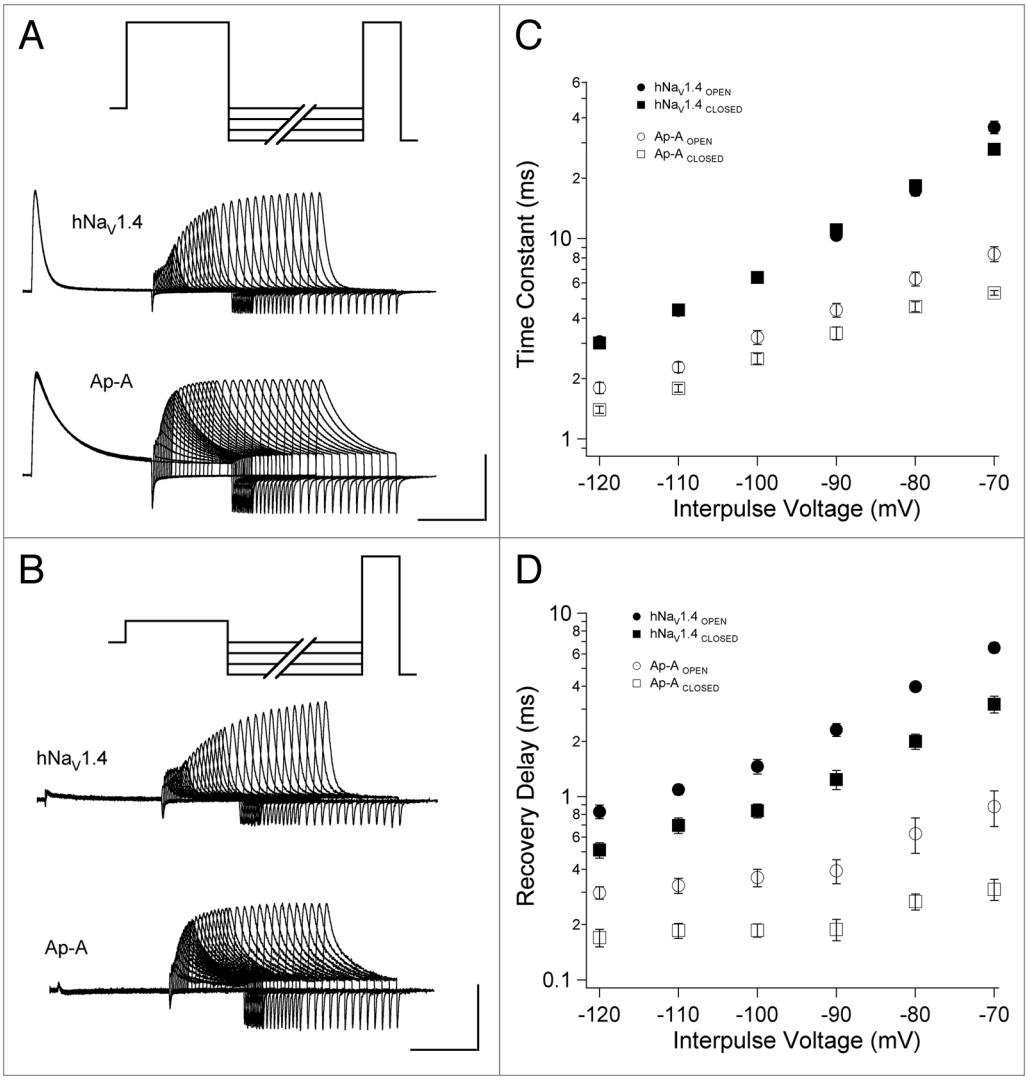

Figure 6. Double pulse protocols used to measure recovery from open-state (A) or closed-state (B) fast inactivation. Recovery traces are shown following -90 mV interpulse commands. Recovery time constants (C) and delays in onset (D) are plotted for naïve or anthopleurin-modified channels. Values represent mean ± SEM for 16 to 20 experiments. Calibration: vertical 500 nA; horizontal 5 ms.

the extent of charge immobilized during open- or closed-state fast inactivation was not significantly altered by anthopleurin. Thus, site-3 toxin produced differential effects on fast inactivation from closed versus open states, but not as a consequence of the magnitude of charge immobilized during these two routes to fast inactivation.

Recovery from fast inactivation. We used double pulse protocols to determine recovery of channel availability following fast inactivation. To promote entry from the open state, channels were depolarized to 0 mV (**Fig. 6A**), and to promote entry from the closed state, channels were depolarized to -40 mV (**Fig. 6B**). For either protocol, variable duration interpulse commands from -120 mV to -70 mV were followed by test pulses to 0 mV to assess channel availability. Time constants of recovery were obtained from normalized recovery curves as detailed in Methods. Recovery from fast inactivation was slightly accelerated in naive channels that inactivated without opening (**Fig. 6C**) but this effect was significant only at -70 mV. Anthopleurin accelerated recovery of channels from fast inactivation compared to naïve channels, at all voltages tested, with mean reduction in time constants at 56.1% (open-state inactivation) and 66.5% (closed-state inactivation). In addition, for anthopleurin-modified channels, recovery was significantly faster for channels inactivating directly from closed versus open states, at all voltages tested.

From these experiments, delay in onset to recovery was determined by fitting the normalized recovery curve with a single exponential function and solving for the x intercept (**Fig. 6D**). Anthopleurin abbreviated recovery delay compared to naive channels, at all voltages tested. The site-3 toxin also decreased the voltage dependence of this first phase of the recovery transition. Recovery delay was significantly abbreviated following inactivation directly from the closed state, compared to open-state fast inactivation, at all voltages tested, for both naïve and anthopleurin-modified channels.

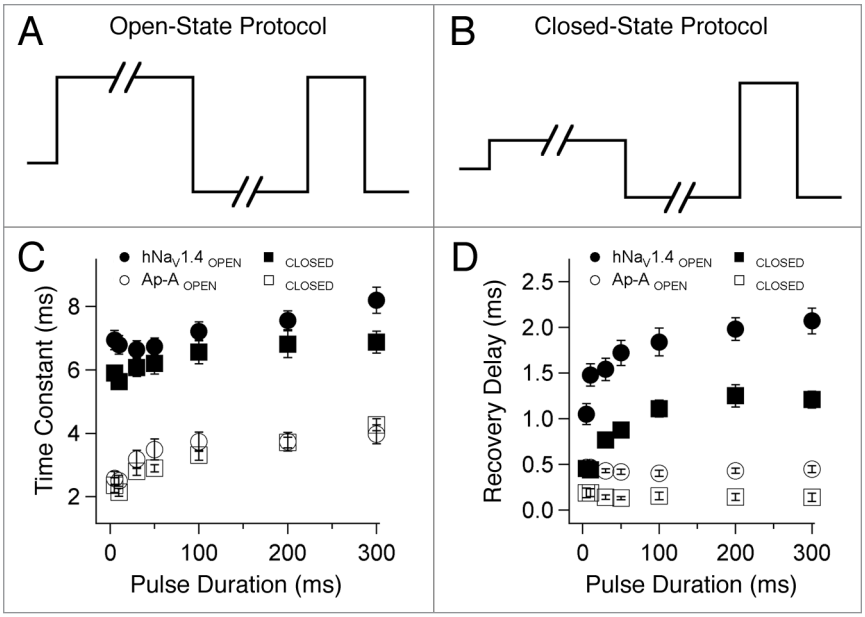

Figure 7. Double pulse protocols used to determine effect of variable-duration inactivating pulses on recovery from open-state (A) or closed-state (B) fast inactivation. Recovery time constants (C) and delays in onset (D) are plotted for naïve or anthopleurin-modified channels. Values represent mean ± SEM for 19 to 24 experiments.

In a separate set of experiments, duration of the initial depolarization was varied from 5 ms to 300 ms to compare recovery and its delay under conditions of increasingly complete inactivation of the channel (**Fig.** 7). These protocols are shown for strong depolarization in **Figure** 7**A** (0 mV, open-state fast inactivation) and for weak depolarization in **Figure** 7**B** (-40 mV, closed-state fast inactivation). Variable duration interpulse commands to -100 mV were used in these experiments.

Recovery was slightly prolonged as duration of the initial depolarization was increased (**Fig.** 7**C**). Recovery was similar for channels inactivating from open versus closed states. For naïve channels, delay to the onset of recovery increased consistently as pulse duration was increased, whereas this effect was absent in anthopleurin-modified channels (**Fig.** 7**D**). Recovery delay was prolonged by 2 to 3 fold in channels inactivating from open versus closed states for either naïve or anthopleurin-modified channels, for inactivating pulse durations up to 300 ms.

Remobilization of gating charge. Double pulse protocols were used to determine parameters of gating charge remobilization in TTX-treated channels inactivated from the open state (0 mV; **Fig. 8A**) or from closed states (-40 mV; **Fig. 9A**). Interpulse commands from -120 mV to -70 mV were followed by 0 mV test pulses to assess the extent of remobilization for each interpulse duration. Integrals for recovering Ig_{ON} were normalized with respect to initial Ig_{ON} of each sweep (open-state) or control Ig_{ON} (closed-state). Each remobilization curve was fit with a double exponential function to determine time constants and fractional amplitudes for the two phases of gating charge remobilization.

In TTX-blocked channels inactivated from the open state, gating charge remobilized with a FAST phase approximately 0.6 ms in duration, followed by a SLOW phase of remobilization with time constants ranging from 4 to 40 ms depending on interpulse voltage (**Fig. 8A**). Anthopleurin significantly accelerated the FAST phase of remobilization at -120 mV, -110 mV and -90 mV, without affecting kinetics of the SLOW phase (**Fig. 8B and C**). Anthopleurin decreased the fractional amplitude of the SLOW phase of charge remobilization at voltages more negative than -80 mV, and attenuated its voltage dependence (**Fig. 8B and D**).

Charge remobilization for channels inactivated at -40 mV (closed-state) is shown in **Figure 9**. Kinetics for FAST and SLOW phases of charge remobilization following closed-state fast inactivation were similar to those observed when 0 mV depolarizing pulses were used (**Fig.** 7). Anthopleurin significantly accelerated the FAST phase of charge remobilization at -120 mV and -110 mV, and had no effect on the kinetics of the SLOW phase of remobilization. TTX-only treated channels exhibited a prominent SLOW phase for charge remobilization (**Fig. 9B and 9D**). At all voltages tested, exposure to toxin significantly decreased the fractional amplitude of the SLOW phase. Thus, anthopleurin elicited similar effects on gating charge remobilization in channels inactivating from open or closed states, to accelerate the kinetics and increase the fractional amplitude of the FAST phase of charge remobilization.

Simulated effect of closed-state fast inactivation on excitability. Our experimental findings showed that closed-state fast inactivation has a significant effect on channel availability in sodium channels. We used computer simulation of skeletal muscle fiber action potentials to test the impact of variable-duration, sub-threshold depolarization on membrane excitability (**Fig. 10**). For simplicity we used single exponential fits to calculate fractional availability of sodium channels as a function of pre-pulse duration (**Fig. 10A**). For each input tested, fractional availability was used to calculate maximal sodium conductance at time of the stimulus to the muscle fiber, as described in Methods. Parameters for skeletal muscle fibers were taken from Cannon et al. and action potentials were simulated by applying depolarizing stimuli from a resting potential of -85 mV.

Control action potentials and responses following conditioning durations of 2 ms, 6.5 ms, 12.5 ms, 22.5 ms, 45 ms and 100 ms are shown for -50 mV (**Fig. 10B**), -60 mV (**Fig. 10C**) and -80 mV input voltages (**Fig. 10D**). Pre-stimulus input to the simulated muscle fibers decreased the amplitude of and increased the time to peak for, simulated action potentials. For example, a 12.5 ms depolarization to -50 mV reduced the action potential by approximately 50% and delayed the time to peak by about 0.5 ms (**Fig. 10B**). At 30% or less channel availability, complete failure of the action potential occurred, with only capacitive responses remaining. Action potential failure was observed with -50 mV inputs of 22.5 ms or longer (**Fig. 10B**) and for -60 mV inputs longer than 100 ms (**Fig. 10C**). With -80 mV inputs for durations

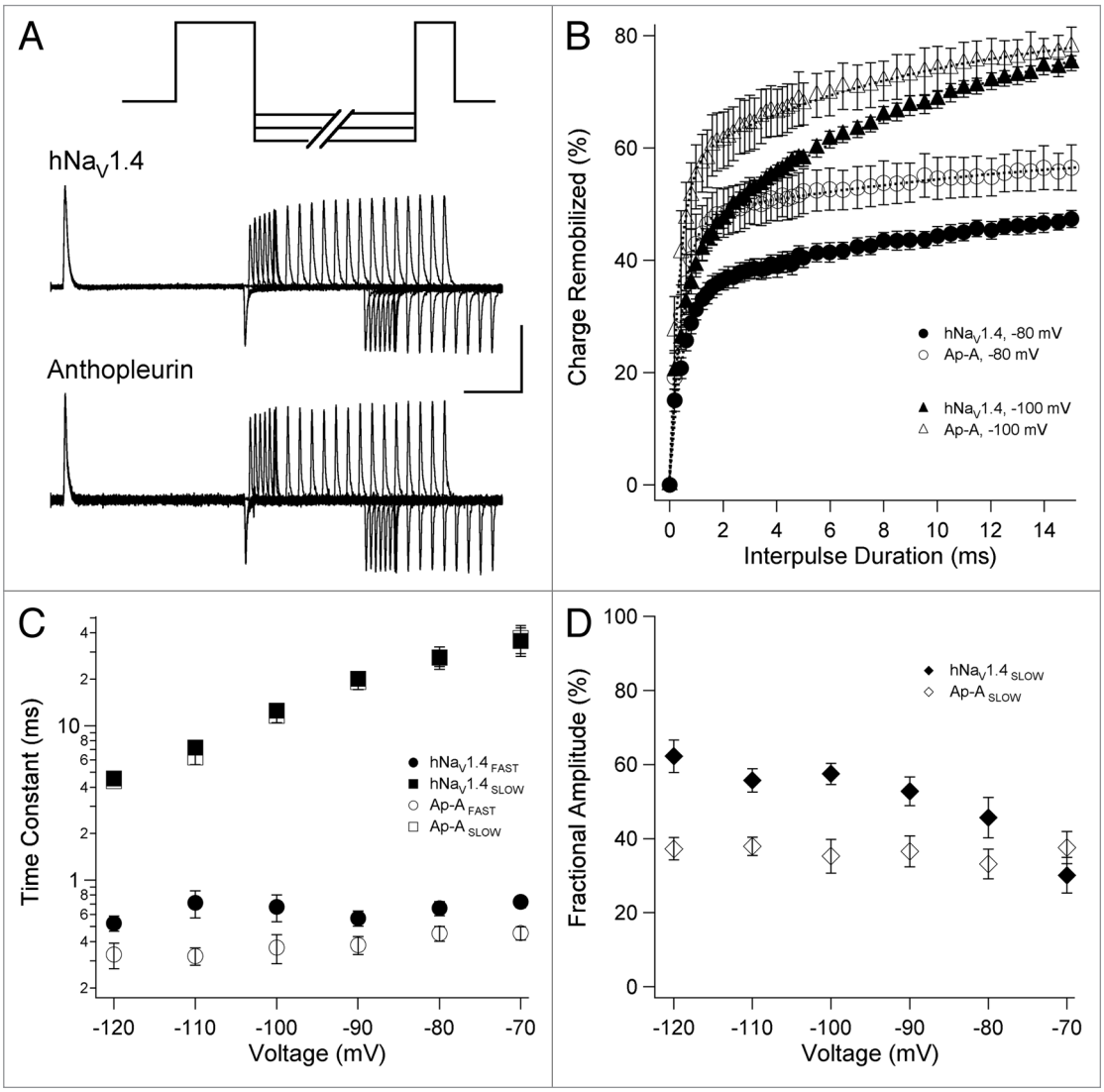

Figure 8. Charge remobilization following open-state fast inactivation; traces are from experiments using -90 mV interpulse commands. In (B) remobilization curves are plotted for select voltages for TTX- (closed symbols) or TTX/anthopleurin-modified (open symbols) channels. These curves were used to calculate parameters of kinetics (C) and fractional amplitudes (D) for FAST and SLOW phases of remobilization. Values represent mean ± SEM for 16 to 20 experiments. Calibration: vertical 200 nA; horizontal 5 ms.

up to 300 ms, only minor changes in the rise time and width of action potentials were observed (**Fig. 10D**).

Discussion

The finding that fast inactivation in the absence of channel opening promotes significant immobilization of the gating charge underscores the functional importance of closed-state fast inactivation to limit recovery of channels. Open- and closed-state routes to fast inactivation are distinguished by their prevalent gating mode, kinetics underlying loss of channel availability, and immobilization of gating charge. In addition, the site-3 toxin anthopleurin-A has differing actions on channels entering into fast inactivation from open versus closed states with respect to these parameters of gating mode, channel availability and charge immobilization. However, recovery of channel availability and remobilization of gating charge are accelerated by site-3 toxin irrespective of route of entry into fast inactivation. The implications of these findings regarding putative functional roles of closed-state fast inactivation and our understanding of the mechanism for sodium channel inactivation are discussed.

Inactivation from open and closed states. Hodgkin and Huxley[32] described the rising phase of the action potential with a model incorporating voltage-dependent activation and inactivation of sodium gating particle permissiveness. Since then several investigations have shown that open-state fast inactivation in sodium channels derives its apparent voltage dependence from the charge displacement of DIVS4.[19,20,33] Current models of sodium channel function describe voltage dependent translocation of S4 segments in domains I to III as requisite for activation and translocation of S4 in domain IV as requisite for binding of the inactivation particle to its receptor.[26,27,34]

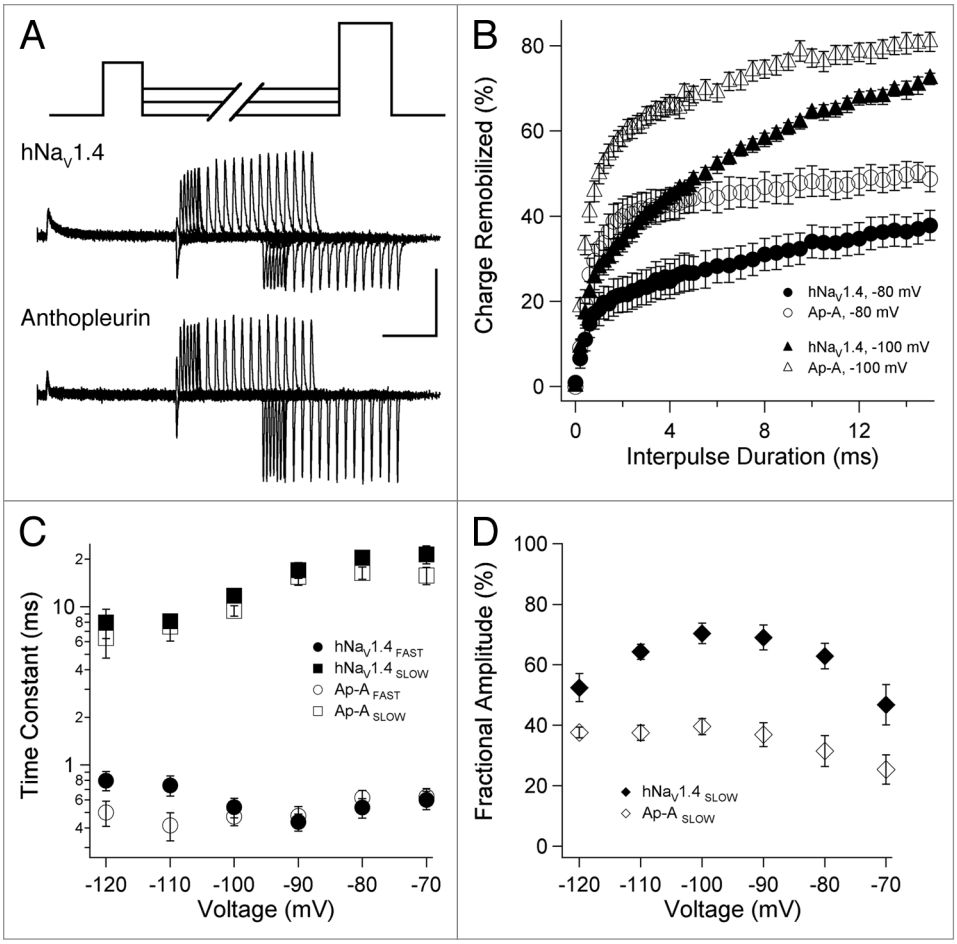

Figure 9. Charge remobilization following closed-state fast inactivation; traces are from experiments using -90 mV interpulse commands. In (B) remobilization curves are plotted for select voltages for TTX- (closed symbols) or TTX-/anthopleurin-modified (open symbols) channels. These curves were used to calculate parameters of kinetics (C) or fractional amplitudes (D) as in Figure 8. Values represent mean ± SEM for 12 to 14 experiments. Calibration: vertical 200 nA; horizontal 5 ms.

Membrane excitability in neurons and muscle fibers is dictated by the fraction of sodium channels available for activation, at a given moment in time. Fast inactivation of sodium channels that have opened to promote the rising phase of an individual action potential limits the frequency of signaling by dictating a relatively short 'refractory' period.[1] By comparison, closed-state fast inactivation in sodium channels has received considerably less attention in studies of excitable cells. After empirically determining the effect of closed-state fast inactivation on sodium channel availability, we tested the impact of closed-state fast inactivation on membrane excitability using computer simulation. Our modeling experiments show that depolarizing inputs that do not activate channels are capable of causing action potential failure in skeletal muscle fibers and support our premise that this form of inactivation can play an important role in the overall regulation of excitability.

Charge immobilization during fast inactivation. We compared charge movement versus immobilization over voltage ranges comprising closed-state versus open-state fast inactivation. Gating charge moves and immobilizes with a steep voltage dependence in response to short, sub-threshold depolarization (-90 mV to -40 mV). This relationship implies that charge movement during closed-state fast inactivation is to a large extent carried by an immobilizable fraction with translocation of DIIIS4 and DIVS4.[23,27] At intermediate voltages (-30 mV to 0 mV), the voltage dependence of charge movement is steep, whereas that for immobilization is shallow. At these voltages charge movement is driving channel activation, with the greatest contribution from non-immobilizable translocations of DIS4 and DIIS4.[26,27] With stronger depolarization (10 mV to 60 mV), both charge movement and its immobilization exhibit a shallow voltage dependence, most likely dominated by the second stage, or late translocation of DIVS4.[29,33]

Stability of the fast-inactivated state is in part the result of immobilization of the gating charge. The gating current observed as voltage sensors respond to step depolarization of membrane potential is asymmetrical with a fast Ig_{ON} component during activation, and two components describing Ig_{OFF} during relaxation of membrane potential. The SLOW component of the OFF gating charge is the result of an immobilization of the gating charge, the onset of which parallels the time course of open-state fast inactivation in squid giant axon.[22] A comparison of charge immobilization during closed-state fast inactivation has not been described until the present report. We have shown that charge immobilized during closed-state transitions with long depolarization is equivalent to that observed with shorter, more positive depolarization and opening of the channel. Closed-state inactivation may provide significant influence on sodium channel function as a consequence of immobilization of the gating charge during closed-state transitions.

Differential effects of anthopleurin-A on fast inactivation. Six classes of neurotoxins with receptor sites on voltage gated sodium channels have been identified.[35] Tetrodotoxin, used in this study to isolate gating currents, binds in the outer vestibule of voltage gated sodium channels, at least in part due to the interaction of its cationic face with aromatic residues there.[36] Gating modifier polypeptide toxins isolated from spiders, scorpions and sea anemones have been used extensively as molecular probes to study structure to function relationships of ion channels. For example, sodium channel isoforms show markedly different affinities to β scorpion toxins that bind to site-4 with receptor sites found in S1-S2 and S3-S4 extracellular linkers of domain II.[37,38] The β scorpion toxins enhance activation, possibly

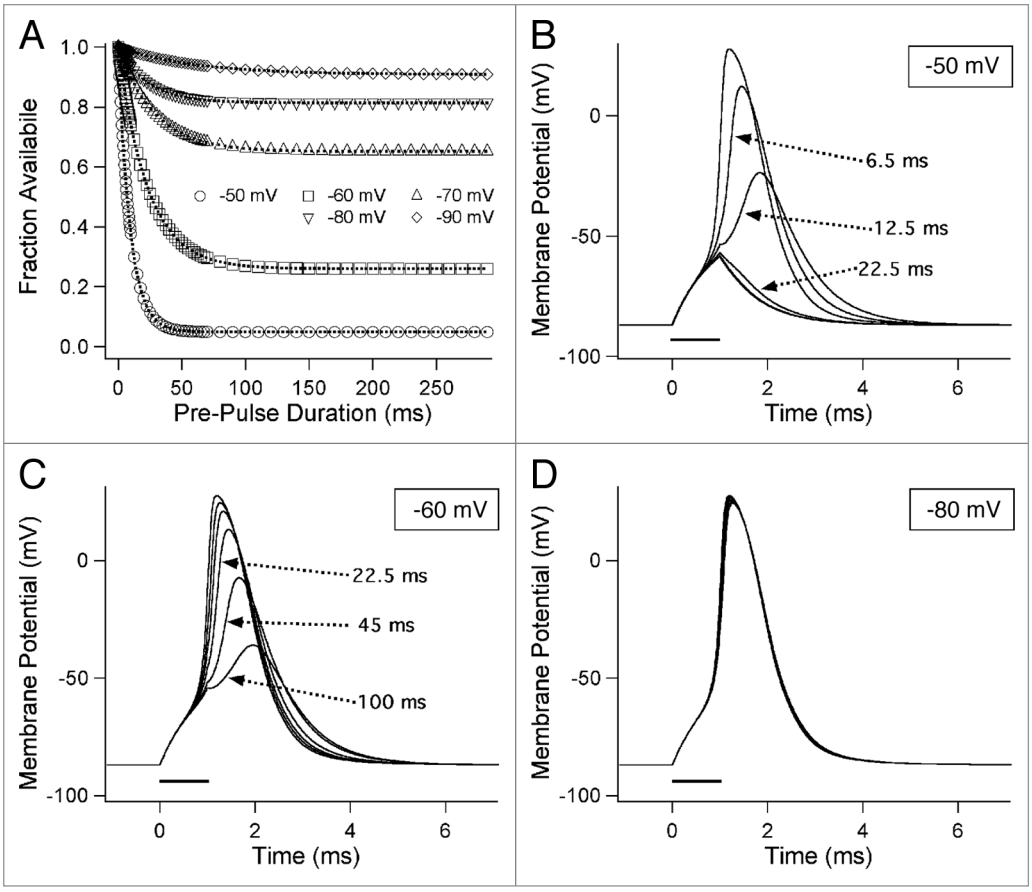

Figure 10. Computer simulation of effect of closed-state fast inactivation on skeletal muscle fiber excitability. (A) Simulated availability curves used to generated weighting factors of sodium conductance at time of stimulus. In (B–D) responses to 1 ms depolarizing stimuli are shown. Pre-stimulus input voltages are indicated in each box.

by 'trapping' DIIS4 in the depolarized favored position. Use of site-4 toxins have supported the notion that DIIS4 translocation is requisite for activation of sodium channels, and that voltage sensor gating is cooperative.[26,39]

Alpha scorpion toxins and anemone toxins have overlapping site-3 receptor sites in the S3-S4 linker of domain IV. Site-3 toxins are, like site-4 toxins, gating modifiers that discriminate among sodium channel isoforms. However, site-3 toxins selectively disrupt sodium channel inactivation.[21] These toxins show preferential affinity for the closed state of the channel.[40,41] Experiments with site-3 toxins have supported the premise that DIVS4 translocation is requisite for fast inactivation of the channel.[29,30,34,41] Alpha scorpion and anemone toxins reduce the total gating charge in cardiac and skeletal muscle sodium channels by approximately 30%,[30,34] presumably by reducing charge movement in DIVS4.

We used the site-3 toxin anthopleurin A as a molecular probe to compare the roles of DIVS4 in open- versus closed state fast inactivation, and on the charge immobilized during those transitions. Our findings identified 3 actions of the toxin that were dependent on the route of entry into a fast-inactivated state. First, anthopleurin slowed open-state fast inactivation, but accelerated inactivation from closed states. Second, anthopoleurin promoted a SLOW gating mode of inactivation of opened channels, but promoted a FAST gating mode of channels inactivating from closed states. Finally, anthopleurin slowed the onset of charge immobilized during open-state fast inactivation, but accelerated immobilization of gating charge in channels that did not open prior to inactivation.

Previous investigations with this toxin using cardiac sodium channels have shown its dramatic effect to slow open-state fast inactivation[42] and reduce the movement of gating charge in response to strong depolarization.[29] These authors also reported a less potent action of anthopleurin to accelerate closed-state fast inactivation at negative membrane potentials.[42] In the present study of skeletal muscle sodium channels, anthopleurin arguably has its most potent kinetic effect on channels inactivating directly from closed states. Nevertheless, we did observe a significant effect of anthopleurin to prolong open-state fast inactivation, and confirmed that this toxin reduces Q_{MAX} in $hNa_V1.4$ to an extent similar to that reported earlier.[29] Therefore, our results are consistent with earlier findings, at least from the perspective that anthopleurin has differential effects on fast inactivation from open and closed states.

It is likely that recording conditions and sodium channel isoform employed have a substantial influence on experimental

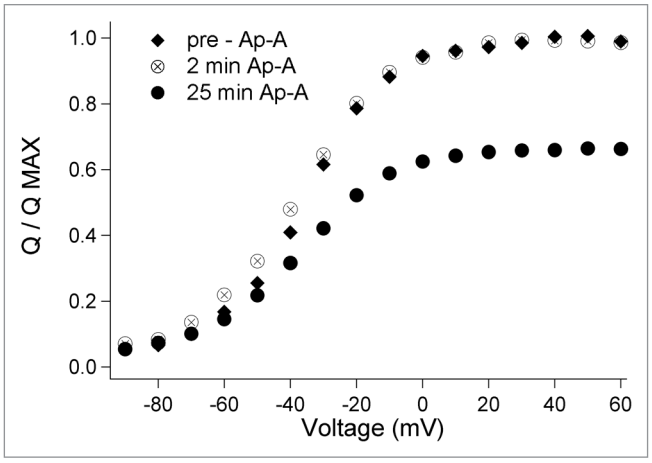

Figure 11. Time course of anthopleurin effect on charge movement in $rNa_V1.4$. Step commands from a holding potential of -120 mV to voltages ranging from -90 mV to 60 mV were delivered at 30 s intervals for 25 min. The effect of anthopleurin on Q/Q_{MAX} prior to exposure, at 2 min, and at 25 min after application are shown. Values represent mean of 5 experiments with error bars removed for clarity.

results obtained with this site-3 toxin. For example, in skeletal muscle sodium channels Q/V relations are left-shifted compared to G/V relations to a greater extent than observed in cardiac sodium channels.[23,29] We determined Q/V midpoint in $hNa_V1.4$ at -40 mV, similar that reported earlier.[23,43] Thus, in studies using cut-open oocyte recordings from $hNa_V1.4$, substantial charge movement is observed during relatively weak depolarizing commands, which is not the case for cardiac channels expressed in mammalian cells.[44] The larger fraction of Q_{MAX} at voltages preceding channel opening may explain the more overt actions of anthopleurin on closed-state transitions in this study compared to previous investigations with this toxin.

Current schemes of sodium channel inactivation for which inactivation from closed states are included, describe a requisite translocation of DIVS4.[26,27] How can this toxin influence DIVS4 to promote inactivation from closed states and yet prohibit open-state inactivation? Perhaps the simplest explanation of differential, state-dependent effects of anthopleurin on fast inactivation is that the site-3 toxin promotes an intermediate position of DIVS4. First, site-3 toxins have greater affinity for the closed state of sodium channels, at negative membrane potential.[40,41] Second, the rate limiting steps to inactivation in the scheme proposed by Armstrong[27] are first stage translocation of DIVS4 (closed-state fast inactivation) and second stage translocation (open-state fast inactivation). Thus, we speculated that the toxin favors stage one translocation with binding at negative membrane potential, but prohibits full translocation of the voltage sensor in response to strong depolarization.

We reasoned that toxin binding might increase gating charge movement during toxin binding, at least until an intermediate position of DIVS4 was established. We tested this hypothesis by monitoring the effect of anthopleurin on Q/Q_{MAX} at 30 sec intervals for 25 min. These measurements (n = 5) were optimized by using the construct $rNa_V1.4$/pGEMHE from which larger gating currents were measured. As shown in **Figure 11**, charge movement (Q/Q_{MAX}) was enhanced early in the time course of toxin exposure, but only at more negative potentials. At 25 min, the effect of anthopleurin was reversed, with a reduction in charge movement at negative voltages. At that time, Q/Q_{MAX} at depolarized potentials was reduced by 34%, similar to our measurements using $hNa_V1.4$/SP64T. Thus, the toxin promotes gating charge movement at negative voltages early in the time course of binding with inhibition of charge movement as binding is complete. We interpret these effects as promotion of DIVS4 towards an intermediate state during toxin binding. As that state is reached, loss of gating charge movement at negative membrane potential reflects the static intermediate position of DIVS4. In other words, some portion of the gating charge associated with first stage DIVS4 translocation is lost with a new resting position of the voltage sensor, promoted by toxin binding. While the interpretation of these findings are consistent with differential actions of anthopleurin on fast inactivation from closed versus open states, other approaches, including fluorescence measurements, are needed to elucidate the precise molecular basis by which this toxin enhances closed-state fast inactivation.

Gating mode of fast inactivation. We found that 500 nM anthopleurin promoted a SLOW gating mode of fast inactivation across the range of open-state fast inactivation. In a previous study of the action of site-3 toxin ATXII on myocytes, bimodal inactivation gating in response to increasing concentration of toxin was attributed to a portioning of unmodified (rapidly inactivating) and modified (slowly inactivating) channels.[45] We found that when concentration of anthopleurin was increased to 1 μM or more, we observed either no change in bimodal gating, or a marked reduction in current amplitude (data not shown). Thus, anthopleurin promotes a SLOW gating mode of fast inactivation in $hNa_V1.4$, as also shown for site-3 α scorpion toxin Ts3, acting on $rNa_V1.4$ (reviewed in ref. 30; PSL Beirao, personal communication). The mechanisms underlying gating mode of fast inactivation are not well understood. However, these findings suggest that site-3 toxins might prove a useful tool in future investigations of inactivation gating mode.

Recovery and remobilization of the gating charge. Following fast inactivation, recovery of channel availability is dictated by the return of voltage sensing S4 segments to their hyperpolarized position, allowing or even promoting the unbinding of the IFMT inactivation particle.[46] Whereas DIS4 and DIIS4 return rapidly to their hyperpolarized-favored positions after inactivation, DIIIS4 and DIVS4 voltage sensors return slowly, as they overcome immobilization of the gating charge encumbered during open-state fast inactivation.[23] Not surprisingly, mutation of voltage sensors in domains III and IV have profound effects on recovery from open-state fast inactivation.[24,47-49] We found that open- and closed-state fast inactivation limit recovery of channels by an equivalent extent, presumably as a consequence of similar efficacies to immobilize the gating charge.

Most sodium channels recover with a voltage-dependent delay suggesting transition through closed states is requisite for channel availability following inactivation.[46] We found that

delay in onset to recovery from fast inactivation is highly dependent on route of entry into the fast-inactivated state. Recovery delay is more rapid for channels inactivating from the closed versus open states. When the duration of the inactivating pre-pulse is increased, the relative difference in recovery delay for channels inactivating from these two states remains constant, for inactivating pre-pulse durations up to 300 ms. These findings suggest that open- and closed-state fast inactivation terminate in separate absorbing states. A limited differential recovery of channels inactivating from closed versus open states most likely is the difference in deactivation time prior to unbinding of the inactivation particle. During open-state fast inactivation, each of the S4 voltage sensors have translocated at least to their activated positions.[27] However, for channels to inactivate without opening, DIS4, DIIS4 or both are still in their deactivated position. Thus, following closed-state fast inactivation, deactivation prior to unbinding of the inactivation particle is more rapid, since at least one of the voltage sensors is already deactivated.

Anthopleurin promotes persistent current in both cardiac and neuronal sodium channels[21,50] and accelerates the recovery of channels inactivating from the open state. In those studies single channel recordings suggest that the effect of the toxin to accelerate recovery is largely independent of an induced persistent current. In $hNa_V1.4$, toxin-promoted persistent current is no larger than that observed in cardiac or neuronal channels, suggesting that the effect of toxin to accelerate recovery is not by promoting transit through the open state. Instead, anthopleurin promotes the FAST phase of charge remobilization, to enhance recovery. This effect is independent of route of entry into fast inactivation. Our findings support the notion that remobilization of DIVS4 drives recovery in skeletal muscle sodium channels, as shown in previous studies of brain[24] and cardiac channels.[25] In addition, they extend this role for DIVS4 remobilization to include recovery from closed-state fast inactivation.

To date, a limited number of studies have investigated closed-state inactivation as a parameter through which sodium channels exert their influence on membrane excitability. Nevertheless, findings from these studies suggest that this route to fast inactivation is relevant from both a physiological and pathological perspective. For example, kinetics of closed-state fast inactivation for $Na_V1.6$ and $Na_V1.7$ dictate firing thresholds in DRG neurons.[51] In terms of pathology, prolonged closed-state fast inactivation may explain the reduced threshold in DRG neurons following axotomy for $Na_V1.3$,[52] and in erythemalgia for $Na_V1.7$.[53] Other studies suggest that defects in this form of fast inactivation contribute to sodium channel dysfunction in muscle channelopathies.[9,10,13,14] Finally, closed-state fast inactivation appears to be crucial for drug interactions with sodium channels.[8,12,54] Our findings show that closed-state fast inactivation promotes significant loss of channel availability and immobilization of the gating charge with depolarization to voltages near threshold, and incurs substantial limitation to recovery. Thus, closed-state fast inactivation should be investigated further as a potential target of drugs, and of mutations that mediate sodium channel dysfunction in ion channel diseases of excitable tissues.

Materials and Methods

Expression of sodium channels in xenopus oocytes. The α subunit of human skeletal muscle sodium channel ($hNa_V1.4$) in vector SP64T was linearized with *EcoR1*. Rat β1 subunit in vector pgh19 was linearized with *HindIII*. Digests were transcribed with SP6 or T3 polymerases using mMessage mMachine kits (Ambion, Austin, TX). For the experiments shown in **Figure 11**, α subunit of rat skeletal muscle sodium channel ($rNa_V1.4$) in vector pGEMHE was linearized with *NheI* and transcribed with T7 polymerase.

Xenopus oocytes were extracted from adult frogs after anesthetizing them in 0.17% tricaine (3-aminobenzoic acid ethyl ester (Sigma Chemical Corp., St. Louis, MO)) according to guidelines approved by the Animal Use and Care Committee at ISU. Individual oocytes were injected with 50 nL RNA at a ratio of 1:3 α/β at 50 nL per oocyte, and cultured with agitation at 18°C in a solution containing 96 mM NaCl, 2 mM KCl, 1.8 mM $CaCl_2$, 1 mM $MgCl_2$, 5 HEPES. 2.5 mM Na pyruvate, with 100 mg/L gentamicin sulfate and 4% horse serum (Hyclone Laboratories, Logan, UT).

Electrophysiology. Recordings were made from oocytes 4 to 8 days after injection. All experiments shown were performed with the cut-open oocyte technique using a Dagan CA1-B amplifier (Dagan Corporation, Minneapolis, MN). The top chamber contained external solution consisting of 120 mM N-methyl D-glucamine, 10 mM HEPES and 2 mM $Ca(OH)_2$, with bottom chamber filled with internal solution of 120 mM N-methyl D-glucamine, 10 mM HEPES and 2 mM EGTA. In some experiments, anthopleurin-A (Sigma) or tetrodotoxin (Alamone Laboratories, Jerusalem, Israel) were added to the top chamber for final concentrations of 500 nM and/or 2 μM, respectively. Temperature of the recording chamber was maintained at 15 ± 0.2°C with a Dagan HC 100A amplifier and Peltier device. Data was obtained using HEKA Pulse 8.67 software (HEKA Instruments, Lambrecht, Germany) at sampling rates of 10 to 50 us per point. Holding potential was -100 mV between trials and -120 mV during protocols.

Steady state relations were determined for activation and fast inactivation. Peak ionic currents in response to step depolarization to voltages ranging from -90 mV to 60 mV were plotted and the I/V parameters of midpoint voltage and slope factor determined from Boltzmann fits according to equation 1:

$$(I/I_{MAX}) = 1/(1 + \exp(-ze_0 (V_M - V_{1/2}) kT)) \quad (1)$$

where I is peak ionic current in response to the test pulse potential V_M, I_{MAX} is the maximum ionic current, z is slope factor, e_0 is elementary charge, $V_{1/2}$ is the midpoint voltage, k is the Boltzmann constant and T is temperature in K. Equation 1 was also used to determine parameters of steady-state fast inactivation. To do this, we used 300 ms conditioning pre-pulse potentials at voltages (V_M) ranging from -120 mV to 20 mV. Channel availability was then assessed with 0 mV test pulses.

Responses to step depolarization to voltages ranging from -40 mV to 40 mV were used to measure kinetics of fast inactivation from the open state. Decline in peak current amplitude at each

voltage was fit with a double exponential function according to equation 2:

$$I(t) = \text{offset} + a_1 \exp(t/\text{tau}_{FAST}) + a_2 \exp(t/\text{tau}_{SLOW}) \quad (2)$$

where offset is the overall asymptote, a_1 and a_2 are asymptotes for the FAST and SLOW components of inactivation, and tau_{FAST} and tau_{SLOW} are time constants. Percent fractional amplitudes of the FAST and SLOW gating modes were calculated as (FAST): $a_1/(a_1 + a_2) * 100$. For parameters of fast inactivation from the closed state, we used pre-pulse potentials at voltages ranging from -90 mV to -40 mV, with variable durations from 0 to 300 ms. Peak current amplitude in response to 0 mV depolarization following each pre-pulse command was measured, and normalized with respect to peak current at time zero. The normalized curve of current decrement was fit with a double exponential function (EQN 2) to determine time constants and fractional amplitudes. Completion of fast inactivation from the closed state was determined from the overall asymptote.

Gating current measurements were performed after treating channels with 2 uM TTX. Charge movement in response to step depolarization was described by a Boltzmann distribution (EQN 1) substituting Q and Q_{MAX} for I and I_{MAX}. Charge immobilization was measured according to equation 3:

$$\%\ \text{charge immobilized} = \{1 - (Ig_{OFF\ FAST}/Ig_{ON})\} * 100 \quad (3)$$

where $Ig_{OFF\ FAST}$ was calculated as the integral of the fast cathodic charge movement during repolarization, and Ig_{ON} was calculated as the total anodic charge movement during depolarization. Onset of charge immobilized during open-state fast inactivation was determined by plotting percent immobilization of gating charge during variable voltage and duration depolarizations over the voltage range of -40 mV to 40 mV. Immobilization curves were fit with a double exponential function (EQN 2) to calculate time constants and fractional amplitudes.

To measure onset of charge immobilized during closed-state fast inactivation, we used the voltage clamp protocol as for ionic current measurements of this state transition. Percent charge immobilization for each pre-pulse depolarization was calculated as

$$\{1 - (Ig_{ON\ TEST}/Ig_{ON\ INITIAL})\} * 100$$

where $Ig_{ON\ TEST}$ and $Ig_{ON\ INITIAL}$ are total Ig_{ON} during the 0 mV TEST following each pre-pulse or at time zero, respectively. For each voltage (-90 mV to -40 mV), the normalized curve of Ig_{ON} gating current loss was plotted as a function of pre-pulse duration. Then, the normalized curve was fit with a double exponential function (EQN 2) to calculate time constants and fractional amplitudes. The maximum charge immobilized during closed-state fast inactivation was calculated from the asymptote of this curve.

Recovery from inactivation was determined with a double pulse protocol in which the first pulse was used to inactivate the channels from the open state (0 mV) or from the closed state (-40 mV). Then, variable voltage and duration hyperpolarizing interpulse commands were used to deactivate channels. Channel availability at the end of each interpulse was assessed by a test pulse to 0 mV. Peak current amplitudes in response to each test pulse were normalized to the initial 0 mV depolarization of each sweep (open-state protocol) or to control 0 mV depolarization (closed-state protocol). The normalized recovery curve was fit with a single exponential curve according to equation 4:

$$I(t) = \text{offset} + a_1 \exp(t/\text{tau}_{REC}) \quad (4)$$

where I(t) is recovery current at time t, offset is the asymptote, a_1 is the current amplitude at the beginning of non-zero recovery, and tau_{REC} is the recovery time constant. The equation was solved for I(t) = 0 to find the x intercept, which was taken as the delay in the onset to recovery from fast inactivation. In some experiments the duration of the inactivating depolarization was varied from 5 ms to 300 ms, for interpulse commands at -100 mV.

Remobilization of the gating charge was determined using the double pulse protocol and interpulse voltages described above, using TTX to block channels. Charge remobilization was assessed by normalizing test Ig_{ON} at each interpulse interval to Ig_{ON} observed with the initial 0 mV pulse (open-state) or with control 0 mV pulses (closed-state). Normalized remobilization curves were fit with a double exponential function according to equation 5:

$$Ig(t) = \text{offset} + a_1 \exp(t/\text{tau}_{REM\ FAST}) + a_2 \exp(t/\text{tau}_{REM\ SLOW}) \quad (5)$$

where Ig(t) is the normalized Ig_{ON} at time t, offset is the overall asymptote, a_1 and a_2 are asymptotes for the FAST and SLOW phases of charge remobilization, and $\text{tau}_{REM\ FAST}$ and $\text{tau}_{REM\ SLOW}$ are the time constants for charge remobilization during those phases. Percent fractional amplitudes of the FAST and SLOW phases of charge remobilization were calculated as (FAST): $a_1/(a_1 + a_2) * 100$.

Data and statistical analyses. Data was analyzed using PulseFit 8.67 and Igor Pro 6.05 (WaveMetrics, Lake Oswego, OR), with statistical analyses performed using Student's t-tests with Instat 2.0 (Graph Pad, San Diego, CA). Statistically significant differences were taken at a criterion of $p \leq 0.05$.

Computer simulation. The effect of closed state inactivation on membrane excitability was simulated for skeletal muscle action potentials, using parameters from Cannon et al.[31] The basic model consists of Na^+ current, a delayed rectifier K^+ current and leak current with constant conductance. Na^+ and K^+ currents were approximated by Hodgkin-Huxley equations. For simplicity, electrical properties of surface and T-tubular membranes were assumed to be identical and K^+ concentration in the T-tubular system was kept constant. We calculated the fractional availability of sodium channels for depolarizing inputs to skeletal muscle fibers. To do this, we used single exponential fits to the normalized kinetic curves shown in **Figure 4A**. These were scaled to 20°C using coefficients from experiments run at 15°C

and 20°C for these same protocols (data not shown, n = 8 to 10 for each conditioning voltage).

Prior to each input tested, maximum Na^+ conductance was reduced by the respective fraction of channels inactivated from the closed-state, as done in earlier studies to incorporate slow inactivation at varied resting potentials.[55] Action potentials were simulated for 1 ms depolarizing stimuli from a resting potential of -85 mV. Simulations were performed using the Runge-Kutta algorithm implemented in the X-Win32 version of XPPAUT (http://www.math.pitt.edu/~bard/xpp/xpp.html) run on a personal computer.

Acknowldegements

We would like to thank Jennifer Abbruzzese (Eccles Cardiovascular Research Training Institute, University of Utah, Salt Lake City, USA) for comments on drafts of this manuscript, and Dr. Steven Cannon (University of Texas SW Medical Center, Dallas, TX) for gift of construct $rNa_V1.4$/pGEMHE. This work was supported by NIH 1R15NSO64556-01 to J.R.G. and by NIH P20 RR016454 to ISU.

References

1. Armstrong CM, Hille B. Voltage-gated ion channels and electrical excitability. Neuron 1998; 20:371-80.
2. Catterall WA. From ionic currents to molecular mechanisms: the structure and function of voltage-gated sodium channels. Neuron 2000; 26:13-25.
3. George AL. Inherited disorders of voltage-gated sodium channels. J Clin Invest 2005; 115:1990-9.
4. Jurkat-Rott K, Lehmann-Horn F. Muscle channelopathies and critical points in functional and genetic studies. J Clin Invest 2005; 115:2000-9.
5. Cannon SC. Pathomechanisms in channelopathies of skeletal muscle and brain. Ann Rev Neurosci 2006; 29:387-415.
6. Bean BP. Sodium channel inactivation in the crayfish giant axon. Must channels open before inactivating? Biophys J 1981; 35:595-614.
7. Aldrich RW, Corey DP, Stevens CF. A reinterpretation of mammalian sodium channel gating based on single channel recording. Nature 1983; 306:436-41.
8. Kambouris NG, Nuss HB, Johns DC, Marban E, Tomaselli GF, Balser JR. A revised view of cardiac sodium channel blockade in the long-QT syndrome. J Clin Invest 2000; 105:1133-40.
9. Chen T, Sheets MF. Enhancement of closed-state inactivation in long QT syndrome sodium channel mutation delta KPQ. Am J Physiol Heart Circ Physiol 2002; 283:966-75.
10. Chen T, Inoue M, Sheets MF. Reduced voltage dependence of inactivation in the SCN5A sodium channel mutation dleF1617. Am J Physiol Heart Circ Physiol 2005; 288:2666-76.
11. Bendahhou S, Cummins TR, Kwiecinski H, Waxman SG, Ptacek LJ. Characterization of a new sodium channel mutatioin at arginine 1,448 associated with moderate paramyotonia congenita in humans. J Physiol 1999; 518:337-44.
12. Mohammadi B, Jurkat-Rott K, Alekov A, Dengler R, Bufler J, Lehmann-Horn F. Preferred mexiletine block of human sodium channels with IVS4 mutations and its pH-dependence. Pharmacogen Genomics 2005; 15:235-44.
13. Wu FF, Gordon E, Hoffman EP, Cannon SC. A C-terminal skeletal muscle sodium channel mutation associated with myotonia disrupts fast inactivation. J Physiol 2005; 565:371-80.
14. Groome JR, Larsen MF, Coonts A. Differential effects of paramyotonia congenita mutants F1473S and F1705I on sodium channel gating. Channels 2008; 2:39-49.
15. Vassilev PM, Scheurer T, Catterall WA. Identification of an intracellular peptide segment involved in sodium channel inactivation. Science 1988; 241:1658-66.
16. West JW, Patton DE, Scheurer T, Wang Y, Goldin AL, Catterall WA. A cluster of hydrophobic amino acid residues required for fast Na^+ channel inactivation. Proc Natl Acad Sci USA 1992; 89:10910-4.
17. Stuhmer W, Conti F, Suzuki H, Wang X, Noda N, Yahagi N, et al. Structural parts involved in activation and inactivation of the sodium channel. Nature 1989; 339:597-604.
18. Noda MS, Shizimu S, Tanabe T, Takai T, Kayano T, Ikeda T, et al. Primary structure of *Electrophorus electricus* sodium channel deduced from cDNA sequence. Nature 1984; 312:121-7.
19. Chahine M, George AL Jr, Zhou M, Ji S, Sun W, Barchi RL, Horn R. Sodium channel mutations in paramyotonia congenita uncouple inactivation from activation. Neuron 1994; 12:281-94.
20. Chen LQ, Santarelli V, Horn R, Kallen RG. A unique role for the S4 segment of domain 4 in the inactivation of sodium channels. J Gen Physiol 1996; 108:549-56.
21. Hanck DA, Sheets MF. Site-3 toxins and cardiac sodium channels. Toxicon 2007; 49:181-93.
22. Armstrong CM, Bezanilla F. Inactivation of the sodium channel. II. Gating current experiments. J Gen Physiol 1977; 70:567-90.
23. Cha A, Ruben PC, George AL Jr, Fujimoto E, Bezanilla F. Voltage sensors in domains III and IV, but not I and II, are immobilized by Na^+ channel fast inactivation. Neuron 1999; 22:73-87.
24. Kuhn FJP, Greef NG. Movement of voltage sensor S4 in domain IV is tightly coupled to sodium channel fast inactivation and gating charge immobilization. J Gen Physiol 1999; 114:167-83.
25. Sheets MF, Kyle JW, Hanck DA. The role of the putative inactivation lid in sodium channel gating current immobilization. J Gen Physiol 2000; 115:609-19.
26. Chanda B, Bezanilla F. Tracking voltage-dependent conformational changes in skeletal muscle sodium channel during activation. J Gen Physiol 2002; 120:629-45.
27. Armstrong CM. Na channel inactivation from open and closed states. Proc Natl Acad Sci USA 2006; 103:17991-6.
28. Groome JR. Charge immobilization from the open and closed states of voltage-gated sodium channels. Biophys Abstr 2009; 248.
29. Sheets MF, Hanck DA. Gating of skeletal and cardiac muscle sodium channels in mammalian cells. J Physiol 1999; 514:425-36.
30. Campos FV, Chanda B, Beirao PSL, Bezanilla F. α scorpion toxin impairs a conformational change that leads to fast inactivation in sodium channels. J Gen Physiol 2008; 251-63.
31. Cannon SC, Brown RH, Corey DP. Theoretical reconstruction of myotonia and paralysis caused by incomplete inactivation of sodium channels. Biophys J 1993; 270-88.
32. Hodgkin AL, Huxley AF. A quantitative description of membrane current and its application to conduction and excitation in nerve. J Physiol 1952; 117:500-44.
33. Horn R, Ding S, Gruber HJ. Immobilizing the moving parts of voltage-gated ion channels. J Gen Physiol 2000; 116:461-75.
34. Sheets MF, Hanck DA. Voltage-dependent open-state inactivation of cardiac sodium channels: gating current studies with Anthopleurin-A. J Gen Physiol 1995; 106:617-40.
35. Catterall WA, Cestele S, Yaorv-Yarovy V, Yu FH, Konoki KK, Scheurer T. Voltage-gated ion channels and gating modifier toxins. Toxicon 2007; 49:124-41.
36. Santarelli VP, Eastwood AL, Dougherty DA, Horn R, Ahern CA. A cation-pi interaction discriminates among sodium channels that are either sensitive or resistant to tetrodotoxin block. J Biol Chem 2007; 282:8044-51.
37. Rogers JC, Qu Y, Tanada TN, Scheurer T, Catterall WA. Molecular determinants of high affinity binding of alpha scorpion toxin and sea anemone toxin in the S3-S4 extracellular loop in domain IV of the Na^+ channel alpha subunit. J Biol Chem 1996: 271:15950-62.
38. Cestele S, Qu Y, Rogers JC, Bochat H, Scheurer T, Catterall WA. Voltage-sensor trapping: enchanced activation of sodium channels by beta-scorpion toxin bound to the S3-S4 loop in domain II. Neuron 1998; 21:919-31.
39. Campos FV, Chana B, Beirao PSL, Bezanilla F. β-scorpion toxin modifies gating transitions in all four voltage sensors of the sodium channel. J Gen Physiol 2007; 130:257-68.
40. Khera PK, Benzinger GR, Lipkind G, Drum CL, Hanck DA, Blumenthal KM. Multiple cationic residues of anthopleurin B that determine high affinity and channel isoform discrimination. Biochem 1995; 34:8533-41.
41. Campos FV, Coronas FIV, Beirao PSL. Voltage-dependent displacement of the scorpion toxin Tx3 from sodium channels and its implication on the control of inactivation. Brit J Pharamacol 2004; 142:1115-22.
42. Hanck DA, Sheets MF. Modification of inactivation in cardiac sodium channels: ionic current studies with anthopleurin-A toxin. J Gen Physiol 1995; 106:601-16.
43. Groome JR, Dice MC, Fujimoto E. Ruben PC. Charge immobilization of skeletal muscle Na^+ channels: role of residues in the inactivation linker. Biophys J 2007; 93:1-15.
44. Sheets MF, Kyle JW, Krueger S, Hanck DA. Optimization of a mammalian expression system for the measurement of sodium channel gating currents. Amer J Physiol 1996; 271:1001-6.
45. El-Sherif N, Fozzard HA, Hanck DA. Dose-dependent modulation of the cardiac sodium channel by sea anemone toxin ATXII. Circ Res 1992; 70:285-301.
46. Kuo CC, Bean BP. Na^+ channels must deactivate to recover from inactivation. Neuron 1994; 12:819-29.
47. Kontis KJ, Goldin AL. Sodium channel inactivation is altered by substitution of voltage sensor positive charges. J Gen Physiol 1997; 110:403-13.
48. Groome JR, Fujimoto E, Walter L, Ruben PC. Outer and central charged residues in DIVS4 of skeletal muscle sodium channels have differing roles in deactivation. Biophys J 2002; 82:1293-307.
49. Groome JR, Alexander HM, Fujiimoto E, Sherry M, Petty D. Central charged residues in DIIIS4 regulate deactivation gating in skeletal muscle sodium channels. Cell Mol Neurobiol 2007; 27:87-106.
50. Benzinger GR, Tonkovich GS, Hanck DA. Augmentation of recovery from inactivation by site-3 Na channel toxins. J Gen Physiol 1999; 113:333-46.
51. Herzog RI, Cummins TR, Ghassemi F, Dib-Hajj SD, Waxman SG. Distinct repriming and closed-state inactivation kinetics of $Na_V1.6$ and $Na_V1.7$ sodium channels in mouse spinal sensory neurons. J Physiol 2003; 551:741-50.

52. Cummins TR, Aglieco F, Renganathan M, Herzog RI, Dib-Hajj SD, Waxman SG. $Na_v1.3$ sodium channels: rapid repriming and slow closed-state inactivation display quantitative differences after expression in a mammalian cell line and in spinal sensory neurons. J Neurosci 2001; 21:5952-61.
53. Cummins TR, Dib-Hajj SD, Waxman SG. Electrophysiological properties of mutant $Na_v1.7$ sodium channels in a painful inherited neuropathy. J Neurosci 2004; 24:8232-6.
54. Nuss HB, Kambouris NG, Marban E, Tomaselli GF, Balser JR. Isoform-specific lidocaine block of sodium channels explained by differences in gating. Biophys J 2000; 78:200-10.
55. Filatov GN, Pinter MJ, Rich MM. Resting potential-dependent regulation of the voltage sensitivity of sodium channel gating in rat skeletal muscle in vivo. J Gen Physiol 2005; 126:161-72.